NICST_MEMO_11_002

NICST Internal Memo

Date: January 31, 2011
From: Jeff McIntire and Sanxiong Xiong
To: Bruce Guenther, Jim Butler, Jack Xiong
Subject: Analysis of the Radiometric Calibration from VIIRS F1 RC-05 Part 2 Test (Nominal Plateau)

References:

[1] 'Sensor Performance Verification Plan,' PVP154640-101.
[2] 'Performance Specification Sensor Specification,' ps154640-101c.
[3] NICST_REPORT_10_087, 'Emissive Band Radiometric Calibration: FU1 RC-05 Part 2 Nominal Plateau,' Jeff McIntire, July 21, 2010.
[4] Y18352, 'Performance Verification Review: Thermal Emissive Band Radiometric Response Characterization (RC-3 and RC-5 Tests),' Eric Johnson and Jim Young, January 18, 2006.
[5] IT_OBCBB_EDU_Temp_081112, 'OBC Blackbody Temperature Calculation,' Courtney Ranshaw, November 11, 2008.
[6] F1_RSR_PVR_JT_091412, 'Performance Verification Report – VIIRS Relative Spectral Response (PVP Section 4.6),' Justin Trice, Nicholas Lardas, and Mark Bliton, December 4, 2009.
[7] Y24182, 'VIIRS FU1 Test Analysis Report fro FP-10 Part 1, Reflective Band Response vs Scan Angle (Version 2),' Courtney Ranshaw, February 19, 2008.
[8] NICST_MEMO_11_001, 'Analysis of the Radiometric Calibration from the VIIRS F1 RC-05 Part 1 Test (Nominal Plateau, Electronic Side B),' Jeff McIntire and Sanxiong Xiong, January 3, 2011.
[9] Y22061, 'VIIRS Test Analysis Report for RC-05, Part 1,' Courtney Ranshaw and Mina Mitani, January 26, 2007.

1. Introduction

The VIIRS F1 thermal vacuum test RC-05 Part 2 was designed to examine the sensor response to the On-Board Calibration (OBC) blackbody in a near space-like environment. This test consisted of two sections: warm up and cool down. The warm up portion was conducted at a series of discrete OBC temperature settings with the OBC temperature controlled over all scans in each collect. For the cool down segment, the OBC temperature was allowed to drift from the highest temperature setting and data was taken at intervals as the OBC temperature decreased.

This work will focus on the radiometric gains and sensitivity as well as on compliance with a number of specifications [1,2]. A preliminary investigation of this test was reported in [3].

Table 1 lists the relevant UAIDs and collects along with their corresponding OBC and Blackbody Calibration Source (BCS) temperatures. The BCS source was located in the last collect window (or at a scan angle of 40.2 degrees). In addition, the Space View Source (SVS) was positioned in the Space View (SV) port.

The VIIRS sensor was operated in diagnostic mode and each collect contains 100 scans. The sensor was set to fixed high gain; as such the low gain state of M13 was not accessed (in addition, the maximum OBC temperature of 315 K is well below the dynamic range for M13 low gain). The test was conducted using electronic side B. The general outline of the methodology used in this work follows from [1,4] with some modifications.

2. Data Processing

The BCS data analyzed here is restricted to a subset of the Earth View (EV) samples in a given collect for which the BCS source yielded a stable response. The following sample ranges were used in this work: samples 1060 – 1319 for M bands and samples 2120 – 2639 for I bands when using the BCS source. All the samples for both the OBC and SV were analyzed.

The DN for the EV sector is truncated to 12 bits while the calibration sectors report DN in 14 bits. This leads to a bias in the dn. As a result, all calibration view data used in this work is truncated to 12 bits.

The response was analyzed using the scan method. First, the DN_{SV} was averaged over all samples in a given scan. Then, the sample averaged DN_{SV} was subtracted from each sample of the DN_{EV} in the corresponding scan to produce the dn. Next, the dn was averaged over samples and the standard deviation of all samples for a specific scan was calculated. Note that the Half Angle Mirror (HAM) sides alternate from scan to scan such that there are 50 scans for each HAM side. Additionally, the I band data is divided into two subsamples; the larger for both SV and OBC is always matched to the larger for the EV, to ensure the proper background subtraction. Lastly, the dn and standard deviation are averaged over scans (each HAM side separately). The same treatment was used for the OBC data to produce the dn_{OBC}.

The temperatures (T_{xxx}) of the following were extracted: BCS, OBC, SVS, HAM, Rotating Telescope Assembly (RTA), scan CAVity (CAV), and OBC blackbody SHield (SH). The OBC, HAM, CAV, and SH temperatures were acquired using the LRV telemetry extractor while the BCS and SVS temperatures were obtained from the Ground Support Equipment (GSE) files. The RTA temperature is the CAV temperature minus 8 degrees K.

Six thermistors within the OBC are used to track the OBC temperature. In addition, three calibration resistors in the back of the OBC are used to correct for self heating effects in the six main thermistors [5].

2.1 Radiometric Calibration

For each of these temperatures, the Planck radiance at a given wavelength is calculated from

$$L_{xxx}\left(C,\lambda,T_{xxx}\left(j_H\right)\right)=\frac{2hc}{\lambda^5}\frac{1}{e^{hc/\lambda kT_{xxx}}-1}. \qquad (1)$$

where C refers to the collect and j_H represents scans (HAM side dependent). The radiance for a particular band and detector is determined by weighting the Planck radiance by the Relative Spectral Response (RSR) over the In Band (IB) region (between the 1% response points), or

$$\left\langle L_{xxx}\left(C,B,D,j_H\right)\right\rangle=\frac{\int_{IB} RSR\left(B,D,\lambda\right)L_{xxx}\left(C,\lambda,T_{xxx}\right)d\lambda}{\int_{IB} RSR\left(B,D,\lambda\right)d\lambda}, \qquad (2)$$

where B and D represent band and detector, respectively. The RSR used here was provided by Raytheon [6].

The effective OBC radiance is

$$\begin{aligned}\left\langle L_{OBC}\left(C,B,D,j_H\right)\right\rangle_{eff} &= \varepsilon_{OBC}\left\langle L_{OBC}\left(C,B,D,j_H\right)\right\rangle \\ &+\left[1-\varepsilon_{OBC}\left(B\right)\right]\left[F_{CAV}\left\langle L_{CAV}\left(C,B,D,j_H\right)\right\rangle\right. \\ &\left.+F_{SH}\left\langle L_{SH}\left(C,B,D,j_H\right)\right\rangle+F_{RTA}\left\langle L_{RTA}\left(C,B,D,j_H\right)\right\rangle\right]\end{aligned}, \qquad (3)$$

where ε_{OBC} is the emissivity of the OBC. F_{CAV}, F_{SH}, and F_{RTA} are the shape factors related to the solid angles of the CAV, SH, and RTA as viewed by the OBC; these factors determine the reflectance off the OBC.

The background radiance contributions from the RTA, HAM, and SVS are defined as

$$\begin{aligned}\left\langle L_{Bkg-yyy}\left(C,B,D,j_H\right)\right\rangle &= rvs\left(B,H,D,\phi_{SVS}\right)\left\langle L_{SVS}\left(C,B,D\right)\right\rangle \\ &-\frac{\left[rvs\left(B,H,D,\phi_{SVS}\right)-rvs\left(B,H,D,\phi_{yyy}\right)\right]}{\rho_{RTA}\left(B\right)} \\ &\times\left[\left\langle L_{HAM}\left(C,B,D,j_H\right)\right\rangle-\left(1-\rho_{RTA}\left(B\right)\right)\left\langle L_{RTA}\left(C,B,D,j_H\right)\right\rangle\right]\end{aligned}. \qquad (4)$$

The yyy refers to either the BCS or OBC, depending on which source is being considered. In addition, the radiances are corrected for Response Versus Scan (RVS) angle and the reflectance factor of the RTA optics (ρ_{RTA}). Note that φ_{yyy} refers to the HAM angle of incidence for the BCS or OBC source (the RVS is normalized to 1 at the OBC HAM angle). The RVS used in this work was provided by Raytheon [7].

Now the scan dependent, background subtracted source radiances are determined by

$$\Delta L_{OBC}\left(C,B,D,j_H\right)=\left\langle L_{OBC}\left(C,B,D,j_H\right)\right\rangle_{eff}-\left\langle L_{Bkg-OBC}\left(C,B,D,j_H\right)\right\rangle, \qquad (5)$$

and

$$\Delta L_{BCS}\left(C,B,D,j_H\right)=\left\langle L_{BCS}\left(C,B,D,j_H\right)\right\rangle-\left\langle L_{Bkg-BCS}\left(C,B,D,j_H\right)\right\rangle. \qquad (6)$$

The background subtracted radiance is modeled by a polynomial in the detector response. These polynomials take the from

$$\Delta L_{OBC}(C,B,D,j_H) = F(B,D,S,j_H)\sum_{i=0}^{N} a_i^{OBC}(B,D,S,j_H)dn_{OBC}^i(C,B,D,S,j_H). \qquad (7)$$

Least-squares fits were performed on a scan by scan basis over the dynamic range at the linear, quadratic, and cubic levels (or order N) to determine the polynomial coefficients. The inverse of the linear term ($1/a_1$) is the radiometric gain (instrument responsivity). The factor F is a cross calibration factor designed to link the calibration of the OBC to the BCS (which is traceable to NIST); this factor is given by

$$F(B,D,S,j_H) = \left\langle \frac{\Delta L_{OBC}(C,B,D,j_H)}{\sum_{i=0}^{N} a_i^{BCS}(B,H,D,S)dn_{OBC}^i(C,B,D,S,j_H)} \right\rangle_C . \qquad (8)$$

where the BCS coefficients were determined from RC-05 Part 1 [8]. For RC-05 Part 2, warm up and cool down were treated separately, and both were fit according to the above procedure. In addition, data for which the SNR was below 1.0 was excluded.

Lastly, the retrieved BCS radiance is defined as [8]

$$\langle L_{BCS}(C,B,D,S,j_H)\rangle_{ret} = \frac{\Delta L_{OBC}(C,B,D,j_H)\sum_{i=0}^{N} a_i^{BCS}(B,H,D,S)dn_{BCS}^i(C,B,H,D,S)}{rvs_{BCS}(B,H,D,\phi_{BCS})\sum_{i=0}^{N} a_i^{BCS}(B,H,D,S)dn_{OBC}^i(C,B,D,S,j_H)} \cdot + \langle L_{Bkg-BCS}(C,B,H,D)\rangle \qquad (9)$$

The retrieved radiance is then averaged over scans. The ratio of the at-detector OBC radiance to the polynomial in OBC dn is a scan by scan correction for linear drift in the coefficients that will be applied on orbit.

2.2 Radiometric Sensitivity

The Signal to Noise Ratio (SNR) is calculated as the ratio of the dn to the standard deviation. This calculation was preformed using the following three methods:

$$SNR_{sample}(C,B,H,D,S) = \frac{1}{M}\sum_{i=0}^{M-1}\frac{dn_{scan}(C,B,H,D,S,i)}{\sigma_{scan}(C,B,H,D,S,i)}, \qquad (10)$$

$$SNR_{scan}(C,B,H,D,S) = \frac{1}{P}\sum_{j=0}^{P-1}\frac{dn_{sample}(C,B,H,D,S,j)}{\sigma_{sample}(C,B,H,D,S,j)}, \qquad (11)$$

and

$$SNR_{overall}(C,B,H,D,S) = \frac{dn_{overall}(C,B,H,D,S)}{\sigma_{overall}(C,B,H,D,S)}, \qquad (12)$$

where the sums are over all extracted samples (M) in a scan and over all extracted scans (P). Eq. (10) describes the sample method, where the SNR is determined over all scans at each sample and then averaged over all extracted samples. Eq. (11) describes the scan method, where the SNR is determined over all extracted samples at each scan and then averaged over all scans. Eq. (12) describes the overall method, where the SNR is determined over all scans and samples simultaneously. The SNR used in this work is the largest of the three (which should be closest to the true sensor SNR).

Next, the SNR is modeled using the following function:

$$\begin{aligned} SNR(C,B,H,D,S) = b_0(B,H,D,S) + b_1(B,H,D,S)\langle L_{OBC}(C,B,H,D,S)\rangle_{ret} \\ + b_2(B,H,D,S)\langle L_{OBC}(C,B,H,D,S)\rangle_{ret}^2 \end{aligned} . \quad (13)$$

The coefficients (b_i) are determined by fitting this function to the data within the dynamic range. In addition, as L_{TYP} for some bands is below the measured range, Eq. (13) was further constrained to include the origin. Eq. (13) is then used to evaluate the SNR at L_{TYP}. For RC-05 Part 2, warm up and cool down were treated separately, and both were fit according to the above procedure. The function used in [8] was difficult to constrain over the limited range of OBC temperatures available during the warm up and cool down cycle.

The Noise Equivalent delta Temperature (NEdT) is the fluctuation in the scene temperature that is equivalent to the system noise; the NEdT is computed via the equation

$$NEdT(C,B,D,H,S) = \frac{NEdL(C,B,H,D,S)}{\frac{\partial L(B,T)}{\partial T}} = \frac{\langle L_{BCS}(C,B,H,D,S)\rangle_{ret}}{SNR(C,B,H,D,S)\frac{\partial L(B,T)}{\partial T}} . \quad (14)$$

The derivative of the Planck radiance with respect to the temperature is evaluated at T_{TYP}. This NEdT is also determined at L_{TYP} using Eq. (13), in order to compare with the specification SRV0053 (listed in Table 3).

2.3 Specifications

The seven specifications that are considered in this memo are listed in Table 3 [2]. The sensitivity requirement was discussed above.

SRV0095, SRV0598, and SRV0654 detail the specifications regarding the OBC operability. SRV0598 states that the OBC must be operable from ambient to 315 K. SRV0095 governs the uniformity of the six thermistors within the OBC; the standard deviation of the six temperatures must be below 0.03 K for temperature controlled conditions (warm up). Lastly, SRV0654 specifies that the OBC must be within ±0.2 K of its commandable setpoints.

The absolute calibration uncertainty is addressed by the following two requirements: SRV0545 and SRV0546. The absolute calibration uncertainty includes all the uncertainties associated with the calibration. This is beyond the scope of this work; however, the fit uncertainty contribution to the absolute uncertainty can be analyzed using the Absolute Radiance Difference (ARD), or

$$ARD_{BCS}(C,B,D,S,j_H) = 100\frac{\langle L_{BCS}(C,B,D,S,j_H)\rangle_{ret} - \langle L_{BCS}(C,B,D,j_H)\rangle}{\langle L_{BCS}(C,B,D,j_H)\rangle} . \quad (15)$$

This is just the percent difference between the retrieved and RSR corrected Planck radiances (essentially, the ARD is a measure of fit uncertainty's effect on the accuracy of the retrieved radiance). This requirement is compared against the values listed in Tables 4 for the specified scene temperatures. These requirements are compared to the ARD at the OBC temperature nearest to the specified scene temperatures.

The final specification (SRV0613) considered here investigates the detector to detector uniformity (or striping). This particular requirement is assessed by means of the Relative Response Uniformity (RRU), or

$$\begin{aligned} RRU_{BCs}(C,B,D,S,j_H) = \max_D \Big(\Big| \langle\langle L_{BCS}(C,B,D,S,j_H)\rangle\rangle_{ret} - \langle L_{BCS}(C,B,D,j_H)\rangle\rangle \\ - \langle\langle\langle L_{BCS}(C,B,D,S,j_H)\rangle\rangle_{ret} - \langle L_{BCS}(C,B,D,j_H)\rangle\rangle\rangle_D \Big| \Big) \\ / \, NEdL(C,B,H,D,S) \end{aligned} \quad , \qquad (16)$$

where the difference between the retrieved radiance and the RSR corrected source radiance is used here. This delta radiance was employed to avoid the large spectral variation from detector to detector produced in the RSR by the spectral smile of the SpMA [9]. Also, note that the measured NEdL is used to compute the RRU. This specification is met if the RRU is less than 1.0 (or the uniformity is within the noise resolution).

3. Analysis

3.1 OBC Operability

The OBC temperature levels measured in this test are plotted in Figure 1. The temperature range is from 273 K to 315 K (in compliance with SRV0598). For Nominal plateau, ambient temperature was about 262 K while the next lowest available OBC setpoint was 273 K. The first eight points in Figure 1 correspond to the first eight collects in Table 1; these collects constitute the warm up part of the cycle in which the OBC temperature was controlled during the full 100 scans of each collect. The last five points in Figure 1 correspond to the last five collects in Table 1; this data makes up the cool down portion of the cycle in which the OBC temperature was allowed to drift from the highest temperature setting and data was taken at intervals. Figure 2 shows the standard deviation over the six thermistors contained in the OBC. Each collect is marked by a different color and each scan within that collect is denoted by a point; the eight collects shown in Figure 2 correspond to the warm up cycle collects in order of ascending OBC temperature. For the warm up cycle, the standard deviation for all scans is below the 0.03 K threshold set by SRV0095. The OBC ssetpoints used for the warm up portion of the cycle are given in Table 5 along with the calculated OBC temperatures. For the lower setpoints, the OBC temperature is outside the ±0.2 K threshold, while the higher setpoints are within the specified limit. The discrepancy is in part the result of the improvement in the OBC temperature calculation described in [5], which was not used in setting the OBC levels during the test.

3.2 Radiometry

The quadratic polynomial fitting for the warm up portion of the cycle is shown in Figure 3 for all high gain bands. Notice that detector 1 in M12 is Out Of Family (OOF). The radiance residual for all bands is shown in Figure 4. The low scene temperatures which resulted in higher residuals in RC-05 Part 1 [8] were not accessed by the OBC; as a result, the residuals are small for all bands (less than 0.1 % for all bands). The fitting for the cool down part of the cycle is shown in Figure 5 for all high gain bands. Again detector 1 in M12 is OOF. Figure 6 shows the radiance residual for the cool down fitting, which is also small (less than 0.1 % for all bands).

The warm up coefficients derived from the quadratic polynomial fits are plotted versus detector in Figures 7 – 9. The equivalent cool down coefficients are graphed in Figures 10 – 12 versus detector. The median detector coefficients are listed in Tables 6 – 8 for both warm up and cool down. The results for HAM side A are consistent with HAM side B. The a_0 coefficients are small (on the order of 10^{-2} or less) for all bands (both warm up and cool down). The a_2 coefficients are also small (on the order of 10^{-8} or less) for all bands (both warm up and cool down). Note that the curvature for the MWIR bands is negative, while the curvature for the LWIR bands is positive. The gains exhibit odd – even dependence in I5, M12, and M13. In addition, the gains for M14 – M16 tend to decrease as the detector number increases. Detector 31 in I5, detector 1 in M12, and detector 8 in M16A are OOF.

The warm up and cool down coefficients are generally consistent. The a_0 terms are small for both; however, for warm up a_0 is consistently larger, sometimes by an order of magnitude. The a_2 coefficients are also consistent. The range over which the fitting is conducted will greatly influence the offset and nonlinear terms; as a result, any comparison must be limited. The gain, however, should be less influenced by the fitting range. The median warm up and cool down gains are different by less than 2 % for all bands (see Table 9).

3.3 Sensitivity and Specifications

The NEdT at T_{TYP} versus detector is shown for all high gain bands in Figures 13 and 14 for warm up and cool down, respectively. The red dashed lines are the specified NEdT at T_{TYP}. All bands and detectors are well below the specified limit for both warm up and cool down. In addition, the warm up and cool down NEdT are consistent. Table 10 lists the median detector NEdT at T_{TYP}.

The worst case detector BCS ARD for all bands is listed in Table 11 for both warm up and cool down (HAM side A). The scene temperatures closest to the specified scene temperatures were compared to the requirements in Table 4; the ARD for all bands met their respective requirements (highlighted in green). The worst case detector ARD is also plotted in Figure 15 for both warm up (solid line) and cool down (dashed line). The LWIR ARD decrease with OBC temperature from about 0.2 % at 273 K to -0.1 % at 315 K during warm up. The cool down LWIR ARD are consistent, albeit slightly larger. The

MWIR ARD are larger than the LWIR (as in Part 1 [8]); the warm up MWIR ARD decrease from roughly 0.5 % at 273 K to 0.2 % at 315 K. The cool down MWIR ARD are larger in magnitude than the warm up by 0.1 – 0.2 %.

The BCS RRU for the worst case detector is shown in Figure 16 for both warm up (solid lines) and cool down (dashed lines). The RRU is also listed in Table 12 for all bands. The RRU is roughly constant (below 0.2) over the measured range of OBC temperatures except for band M14, which increases to approximately 0.7 at 315 K. These results are consistent between warm up and cool down. Note that the specified limit for the detector uniformity is 1.0; as a result, all bands are within the specified limits on striping for this temperature range.

4. Summary

- The OBC was operated over a temperature range from ambient to 315 K.
- The uniformity of the six thermistors within the OBC was within 0.03 K.
- The OBC temperature was not within the specified tolerance (±0.2 K) for the lowest setpoints. Discrepancy possibly due to improvement in OBC temperature calculation not being used in setting OBC temperature during testing.
- The linear coefficient a_1 dominates the relationship between radiance and response.
- Warm up and cool down gains are comparable to within 2 %.
- The a_0 coefficient is small (on the order of 10^{-2} or less).
- The a_2 coefficient is also small (on the order of 10^{-8} or less). The curvature of the MWIR bands is negative, while the curvature of the LWIR bands is positive.
- The NEdT at T_{TYP} is within the specified resolution for all bands and detectors.
- The retrieved radiance is within the specified accuracy at all relevant specified scene temperatures.
- Detector to detector striping is within the noise resolution for all bands and detectors.

Acknowledgement

The sensor test data used in this document was provided by the Raytheon El Segundo testing team. Approaches for data acquisition and data reductions, as well as data extraction tools were also provided by the Raytheon El Segundo team. We would like to thank the Raytheon El Segundo team for their support. The data analysis tools were developed by the NICST team.

Table 1: F1 RC-05 Part 2 data (Nominal plateau)

UAID	Collect	OBC Temperature (K)	BCS Temperature (K)
U3103908	1	273.0	300.1
U3103908	2	282.9	300.1
U3103908	3	292.8	300.1
U3103908	4	297.7	300.1
U3103908	5	302.6	300.1
U3103908	6	307.5	300.1
U3103908	7	312.5	300.1
U3103908	8	314.9	300.1
U3103908	9	312.0	300.1
U3103908	10	307.1	300.1
U3103908	11	302.2	300.1
U3103908	12	297.3	300.1
U3103908	13	292.5	300.1

Table 2: Specifications addressed by this work [2]

SRV0053	The VIIRS sensor emissive bands shall meet the sensitivity requirments of TABLE 15. (TABLE 15 is listed as Table 3 in this text.)
SRV0545	For the bands specified as moderate resolution and emissive, the absolute radiometric calibration uncertainty of spectral radiance shall be equal to or less than the percentage specified in TABLE 17. (TABLE 17 is listed as Table 4 in this text.)
SRV0546	For the bands specified as imaging and emissive (TABLE 1), given a uniform scene of brightness temperature of 267 K, the calibration uncertainty of spectral radiance shall be as specified in TABLE 18. (TABLE 18 is listed as Table 4 in this text.)
SRV0613	The calibrated output of all channels within a band shall be matched to the band mean output within the NEdL / NEdT (1 sigma) when viewing a uniform scene. The matching condition shall be met between radiance levels from L_{MIN} to 0.9 L_{MAX}.
SRV0598	The sensor shall be capable of controlling the temperature of the on-board blackbody to a commamdable setpoint between approximately ambient and 315 K.
SRV0654	The sensor shall be capable of maintianing the temperature of the on-board blackbody to within ±0.2 K of the programmed setpoint temperature.
SRV0095	The emitting surface of the VIIRS sensor on-board blackbody source shall have a temperature uniformity of 0.03 K when operated under temperature controlled or unpowered conditions. Temperature uniformity is defined as the standard deviation of the temperatures measured by the sensors embbedded in the OBC BB.

Table 3: Sensitivity requirements for the emissive bands [2]

			Single Gain		Dual Gain			
					High Gain		Low Gain	
Band	Center Wavelength (nm)	Gain Type	T_{TYP}	NEdT	T_{TYP}	NEdT	T_{TYP}	NEdT
M12	3700	Single	270	0.396	~	~	~	~
M13	4050	Dual	~	~	300	0.107	380	0.423
M14	8550	Single	270	0.091	~	~	~	~
M15	10783	Single	300	0.07	~	~	~	~
M16	12013	Single	300	0.072	~	~	~	~
I4	3740	Single	270	2.5	~	~	~	~
I5	11450	Single	210	1.5	~	~	~	~

Table 4: Absolute radiometric calibration uncertainty of the spectral radiance for the emissive bands [2]

Band	Scene Temperature (K)					
	190	230	267	270	310	340
I4	~	~	5.00%	~	~	~
I5	~	~	2.50%	~	~	~
M12	N/A	7.00%	~	0.70%	0.70%	0.70%
M13	N/A	5.70%	~	0.70%	0.70%	0.70%
M14	12.30%	2.40%	~	0.60%	0.40%	0.50%
M15	2.10%	0.60%	~	0.40%	0.40%	0.40%
M16	1.60%	0.60%	~	0.40%	0.40%	0.40%

Table 5: OBC average temperatures and commanded setpoints

Collect	OBC set point (K)	OBC T (K)
1	272.5	273.0
2	282.5	282.9
3	292.5	292.8
4	297.5	297.7
5	302.5	302.6
6	307.5	307.5
7	312.5	312.5
8	315.0	314.9

Table 6: Median a_0 coefficient for all thermal bands

Band	Warm Up		Cool Down	
	HAM A	HAM B	HAM A	HAM B
I4	8.99E-04	8.74E-04	5.15E-04	3.77E-04
I5	3.00E-02	3.20E-02	-9.93E-03	-7.05E-03
M12	1.99E-04	1.82E-04	-2.69E-04	-4.92E-04
M13 HG	-1.60E-04	-4.88E-05	-1.18E-03	-1.45E-03
M14	5.60E-02	6.17E-02	9.67E-03	1.75E-02
M15	2.69E-02	2.82E-02	4.43E-03	-2.81E-03
M16A	4.12E-02	4.04E-02	-3.80E-03	-6.30E-03
M16B	4.03E-02	3.74E-02	4.52E-04	-1.11E-02

Table 7: Median a_1 coefficient for all thermal bands

Band	Warm Up		Cool Down	
	HAM A	HAM B	HAM A	HAM B
I4	8.88E-04	8.89E-04	8.92E-04	8.93E-04
I5	5.67E-03	5.67E-03	5.73E-03	5.78E-03
M12	8.22E-04	8.22E-04	8.26E-04	8.26E-04
M13 HG	1.67E-03	1.67E-03	1.68E-03	1.68E-03
M14	5.08E-03	5.11E-03	5.11E-03	5.14E-03
M15	5.59E-03	5.61E-03	5.64E-03	5.65E-03
M16A	4.85E-03	4.86E-03	4.92E-03	4.94E-03
M16B	4.85E-03	4.86E-03	4.95E-03	4.95E-03

Table 8: Median a_2 coefficient for all thermal bands

Band	Warm Up		Cool Down	
	HAM A	HAM B	HAM A	HAM B
I4	-4.96E-09	-5.14E-09	-5.97E-09	-6.06E-09
I5	2.22E-08	2.36E-08	2.09E-09	3.13E-09
M12	-1.02E-09	-1.13E-09	-1.44E-09	-1.97E-09
M13 HG	-1.37E-08	-1.29E-08	-1.54E-08	-1.57E-08
M14	7.14E-08	7.22E-08	5.10E-08	5.07E-08
M15	2.11E-08	2.33E-08	1.10E-08	1.07E-08
M16A	2.95E-08	2.93E-08	9.70E-09	1.11E-08
M16B	3.01E-08	2.94E-08	1.30E-08	1.06E-08

Table 9: Median gain for all thermal bands

Band	Warm Up		Cool Down	
	HAM A	HAM B	HAM A	HAM B
I4	1123.1	1122.7	1118.8	1118.5
I5	174.6	174.3	172.7	172.4
M12	1175.8	1174.9	1169.9	1168.3
M13 HG	598.8	598.6	596.0	595.4
M14	197.4	196.2	194.2	193.0
M15	178.4	177.8	177.2	176.5
M16A	206.0	205.6	202.8	202.2
M16B	205.6	205.1	202.8	202.4

Table 10: Median NEdT at T_{TYP} for all thermal bands

Band	Warm Up		Cool Down		Spec
	HAM A	HAM B	HAM A	HAM B	
I4	0.406	0.407	0.420	0.422	2.5
I5	0.385	0.393	0.389	0.411	1.5
M12	0.119	0.120	0.131	0.131	0.396
M13 HG	0.044	0.044	0.043	0.043	0.107
M14	0.056	0.056	0.054	0.056	0.091
M15	0.029	0.029	0.028	0.029	0.070
M16A	0.037	0.037	0.037	0.037	0.072
M16B	0.037	0.037	0.038	0.038	0.072

Table 11: BCS ARD worst case detector for HAM side A

	OBC T (K)	I4	I5	M12	M13 HG	M14	M15	M16A	M16B
warm up	273.0	0.60	0.11	0.36	0.29	0.21	0.12	0.11	0.10
warm up	282.9	0.38	0.04	0.35	0.28	0.09	0.04	0.05	0.05
warm up	292.8	0.36	-0.01	0.25	0.29	0.03	0.00	0.01	0.01
warm up	297.7	0.32	-0.02	0.23	0.28	0.01	-0.03	-0.01	0.00
warm up	302.6	0.19	-0.05	0.23	0.23	-0.03	-0.05	-0.03	-0.03
warm up	307.5	0.16	-0.08	0.26	0.18	-0.06	-0.08	-0.05	-0.04
warm up	312.5	0.09	-0.09	0.22	0.12	-0.07	-0.09	-0.06	-0.05
warm up	314.9	0.10	-0.10	0.22	0.08	-0.08	-0.10	-0.06	-0.05
cool down	312.0	0.25	-0.03	0.44	0.30	-0.01	-0.04	-0.01	0.00
cool down	307.1	0.34	-0.01	0.43	0.35	0.02	-0.01	0.02	0.02
cool down	302.2	0.38	0.01	0.43	0.39	0.05	0.00	0.02	0.03
cool down	297.3	0.43	0.03	0.40	0.40	0.06	0.01	0.04	0.05
cool down	292.5	0.47	0.04	0.40	0.40	0.09	0.04	0.05	0.06

Table 12: BCS RRU worst case detector for HAM side A

	OBC T (K)	I4	I5	M12	M13 HG	M14	M15	M16A	M16B
warm up	273.0	0.06	0.06	0.12	0.13	0.19	0.18	0.13	0.17
warm up	282.9	0.03	0.05	0.12	0.13	0.32	0.27	0.24	0.13
warm up	292.8	0.02	0.04	0.11	0.13	0.37	0.24	0.18	0.21
warm up	297.7	0.02	0.05	0.09	0.11	0.43	0.25	0.15	0.14
warm up	302.6	0.02	0.06	0.10	0.09	0.54	0.20	0.15	0.17
warm up	307.5	0.02	0.04	0.08	0.09	0.54	0.25	0.16	0.16
warm up	312.5	0.02	0.04	0.13	0.12	0.52	0.23	0.17	0.19
warm up	314.9	0.03	0.05	0.12	0.09	0.67	0.18	0.16	0.20
cool down	312.0	0.03	0.06	0.08	0.09	0.51	0.21	0.18	0.16
cool down	307.1	0.02	0.06	0.08	0.09	0.41	0.22	0.14	0.14
cool down	302.2	0.02	0.04	0.03	0.08	0.41	0.21	0.16	0.16
cool down	297.3	0.02	0.04	0.04	0.10	0.43	0.14	0.12	0.13
cool down	292.5	0.03	0.04	0.06	0.12	0.39	0.19	0.14	0.17

Figure 1: OBC temperature range

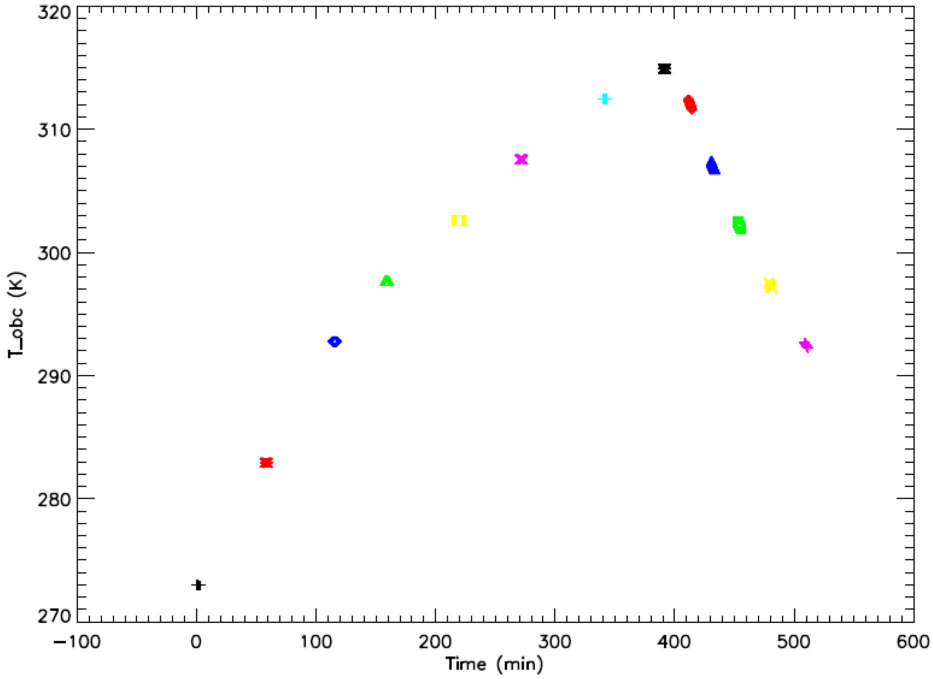

Figure 2: Standard deviation of OBC thermistors

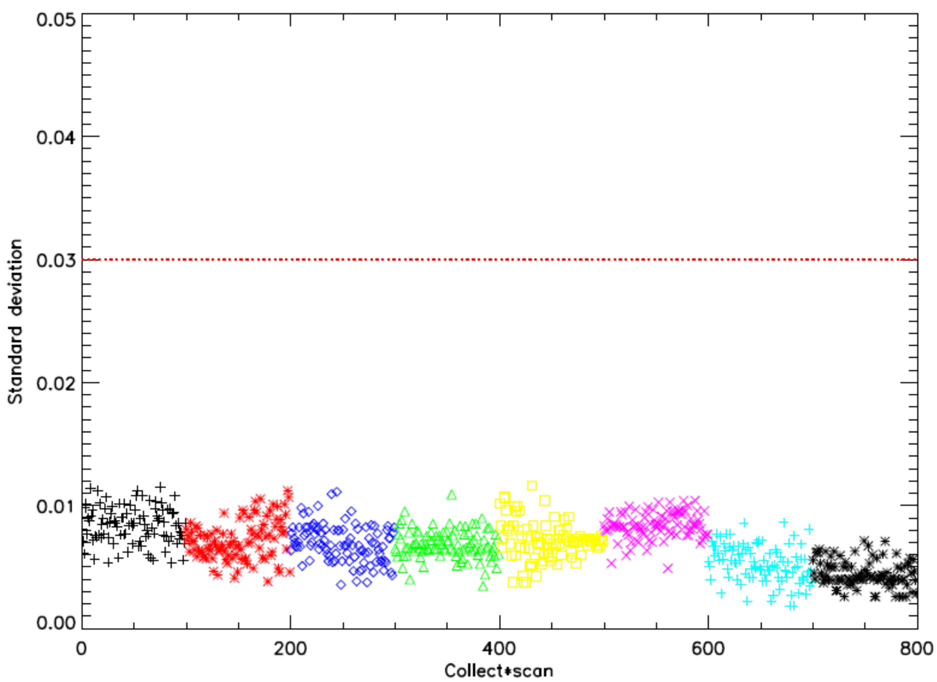

Figure 3: ΔL_{OBC} versus dn for all high gain bands (warm up)

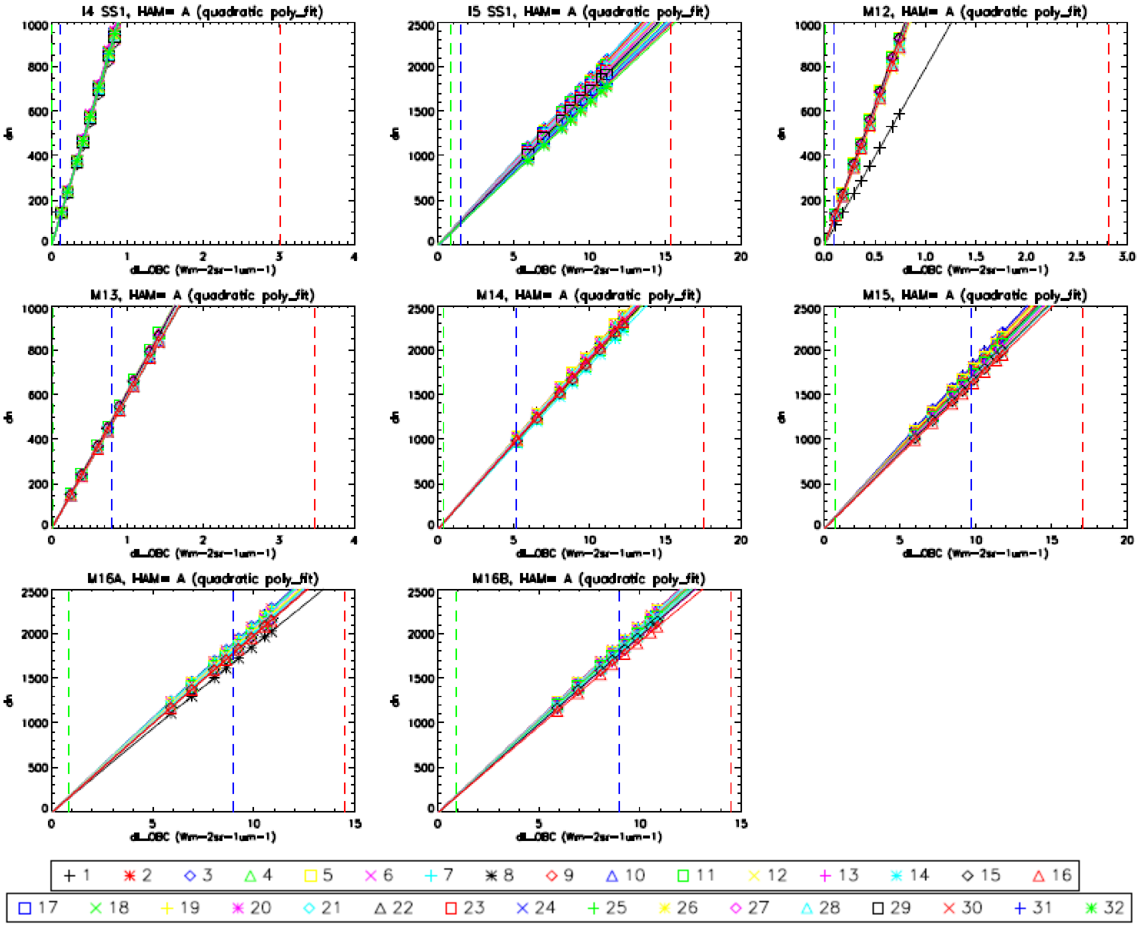

Figure 4: radiance residual for all high gain bands (warm up)

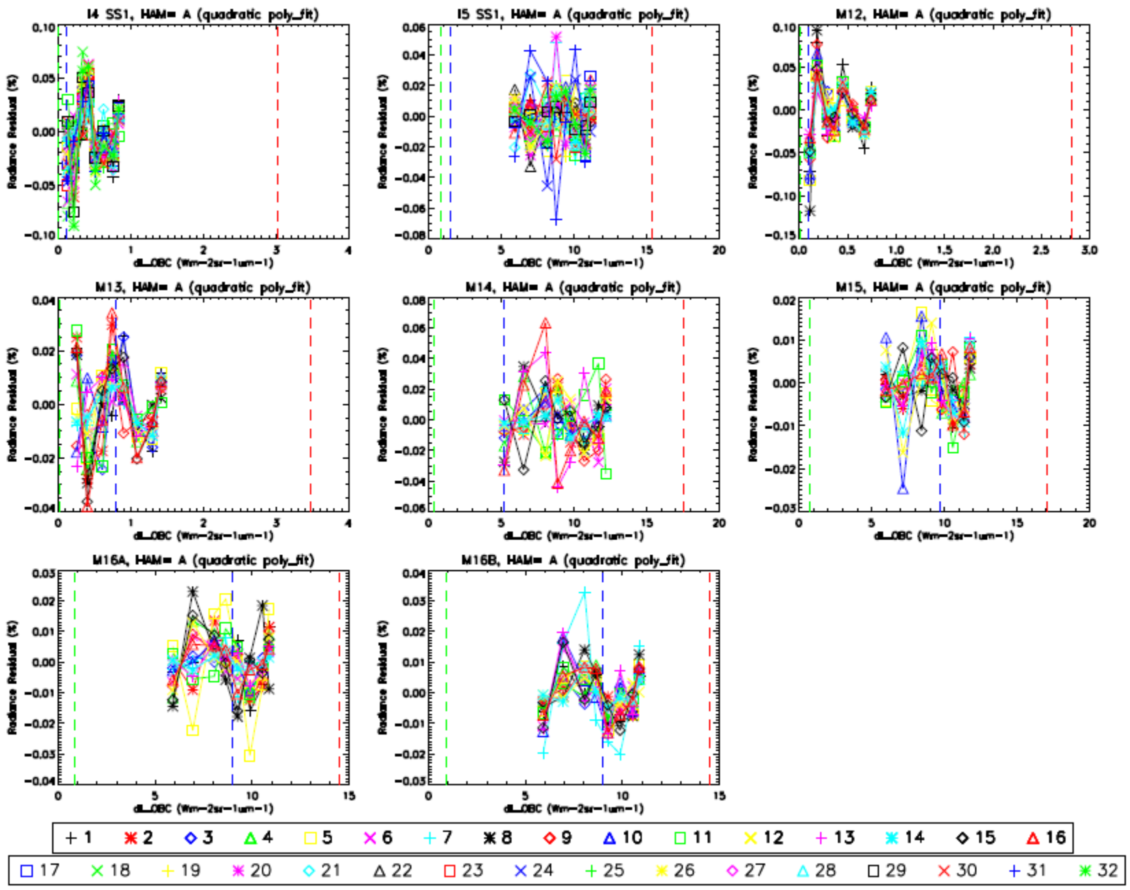

Figure 5: ΔL_{OBC} versus dn for all high gain bands (cool down)

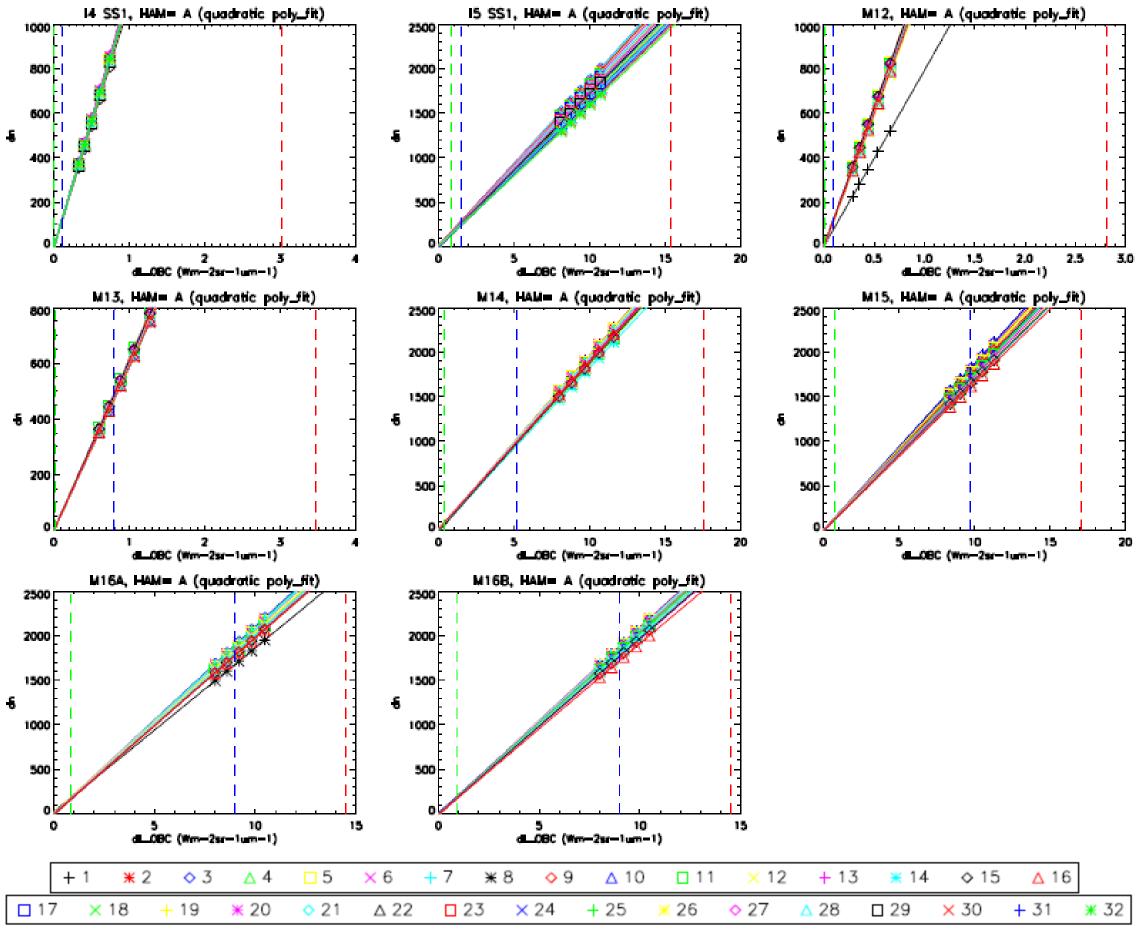

Figure 6: radiance residual for all high gain bands (cool down)

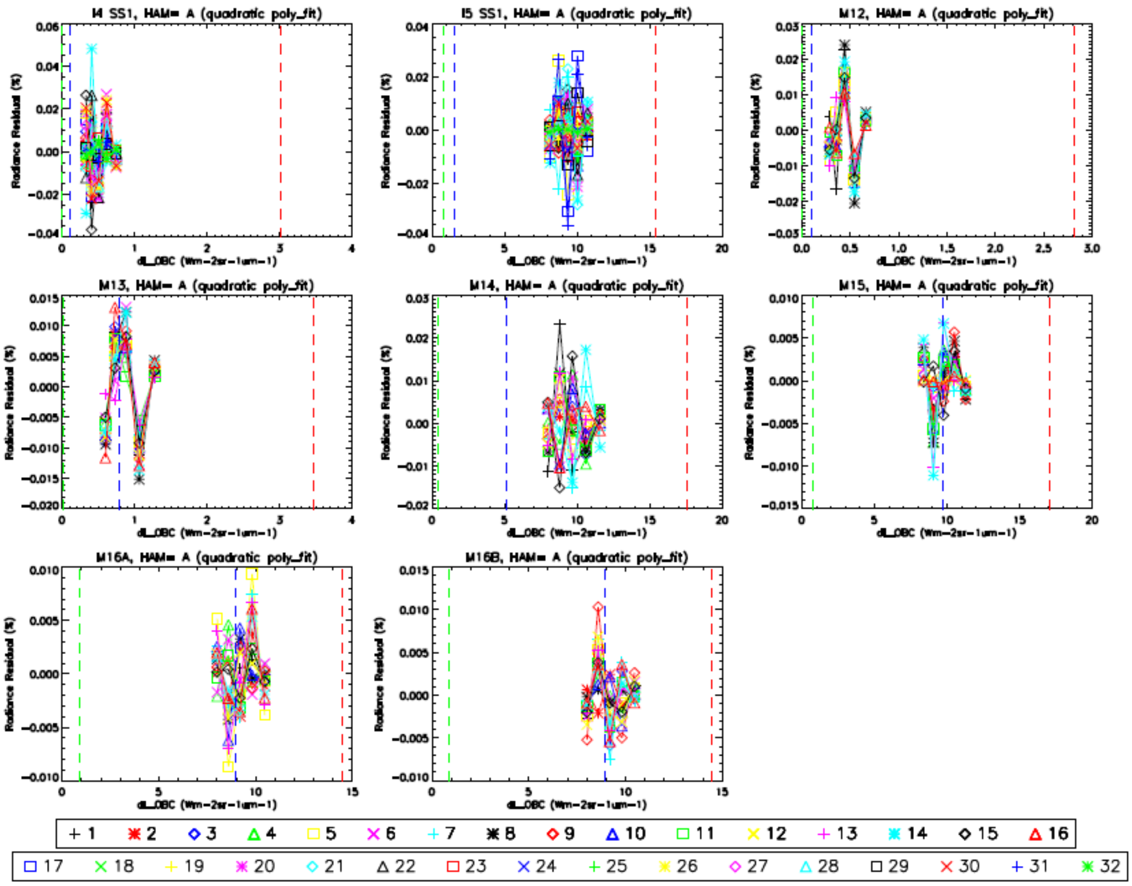

Figure 7: a_0 coefficient for high gain bands (warm up)

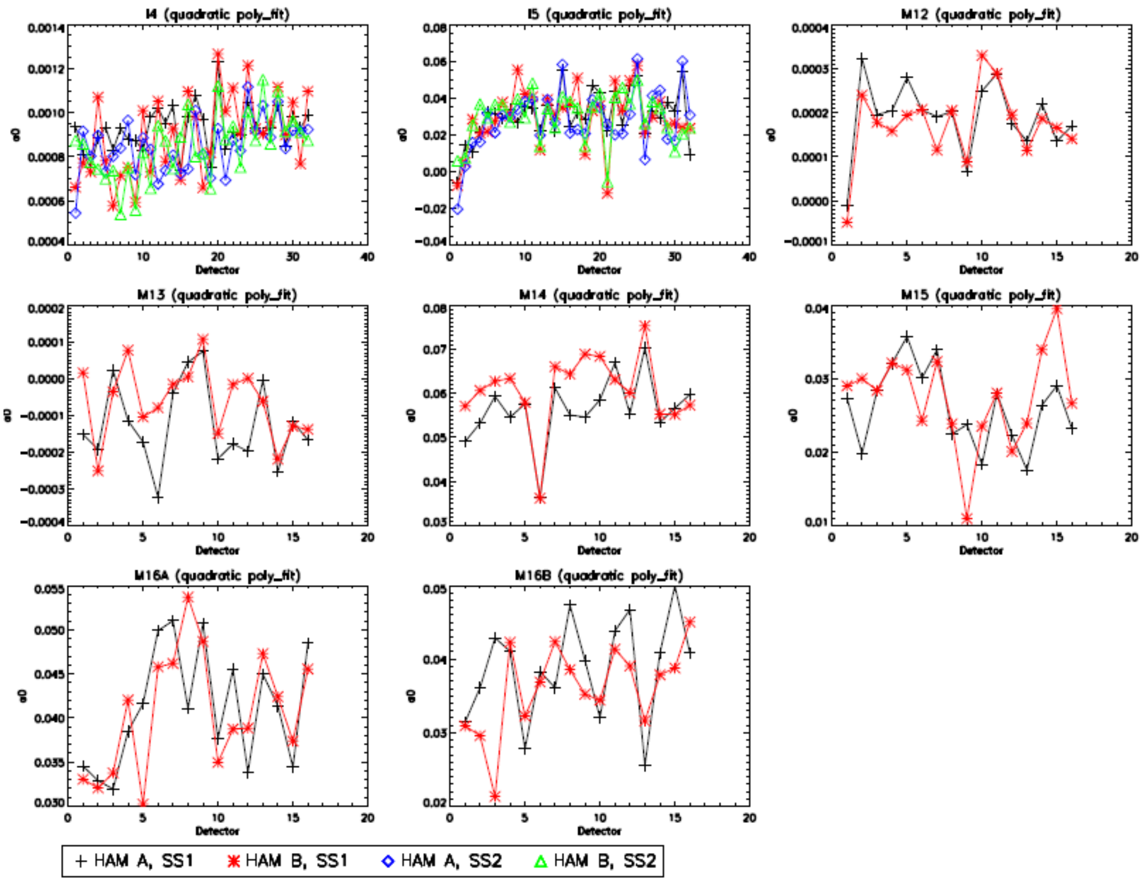

Figure 8: gain ($1/a_1$) for high gain bands (warm up)

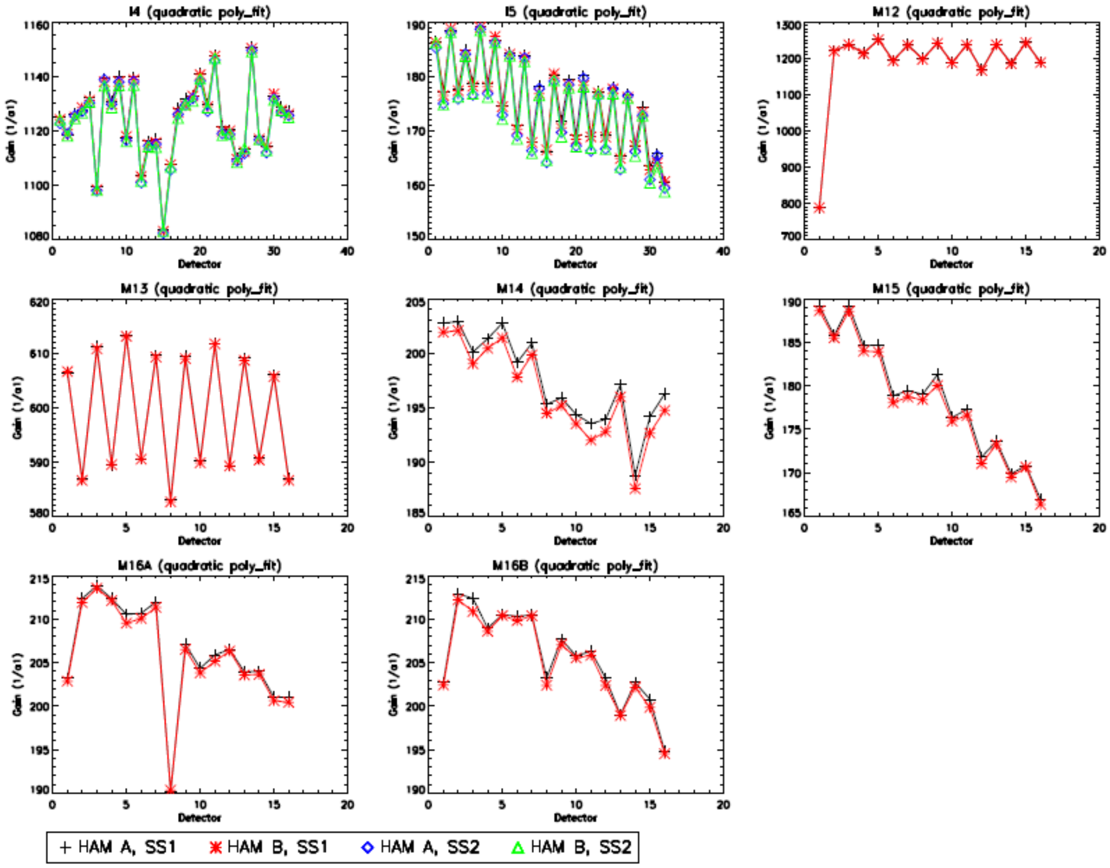

Figure 9: a_2 coefficient for high gain bands (warm up)

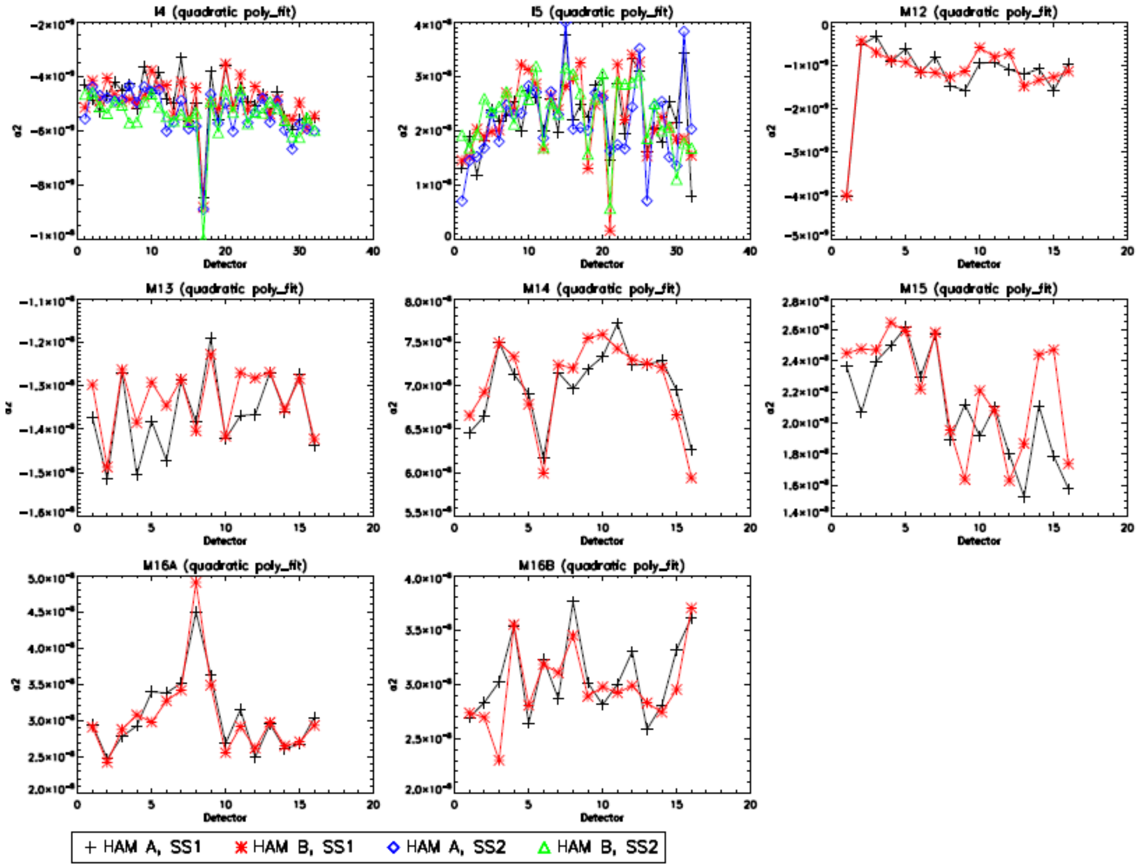

Figure 10: a_0 coefficient for high gain bands (cool down)

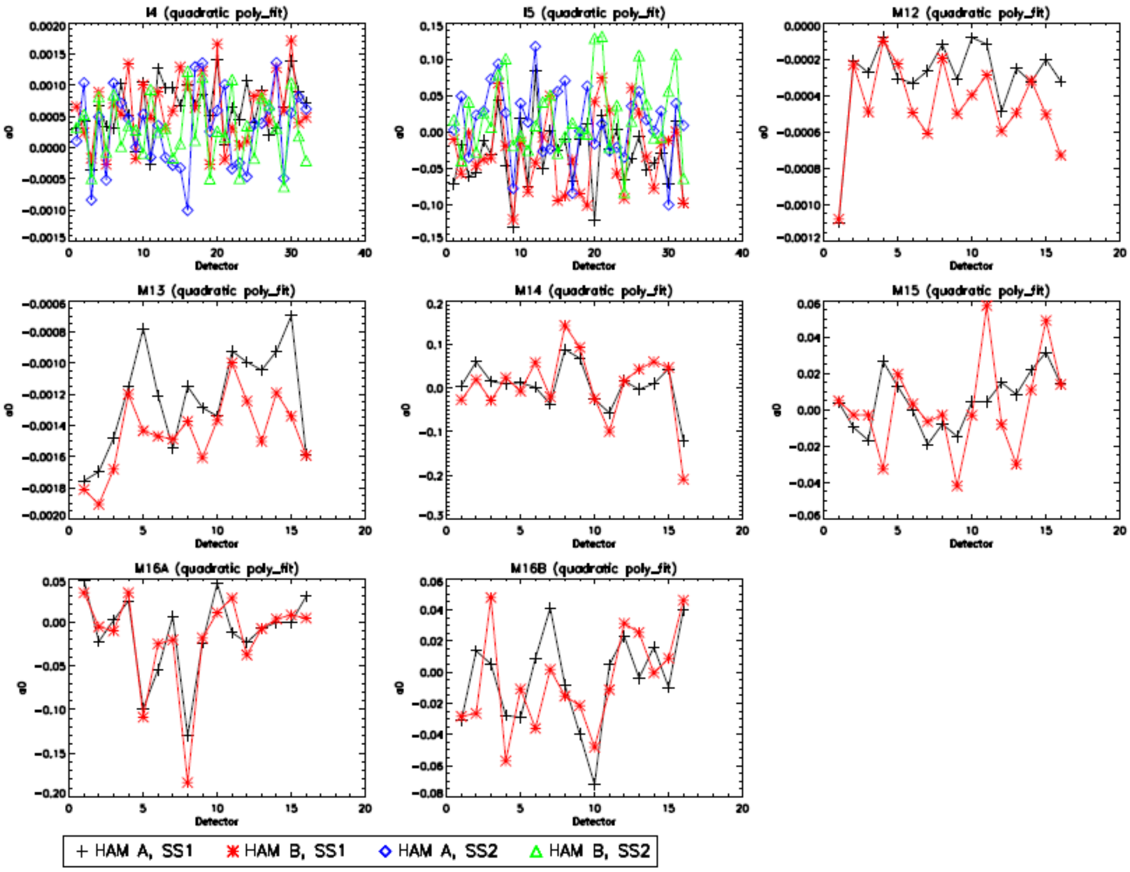

Figure 11: gain ($1/a_1$) for high gain bands (cool down)

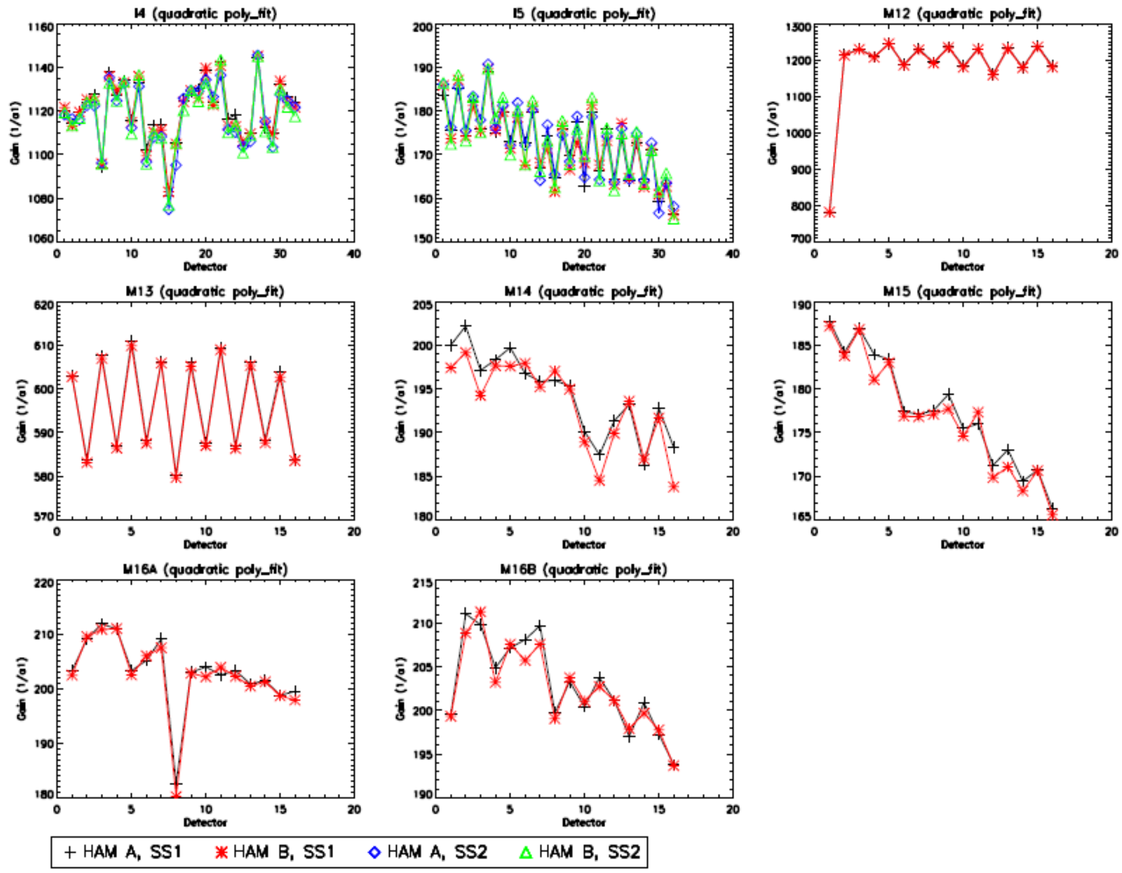

Figure 12: a_2 coefficient for high gain bands (cool down)

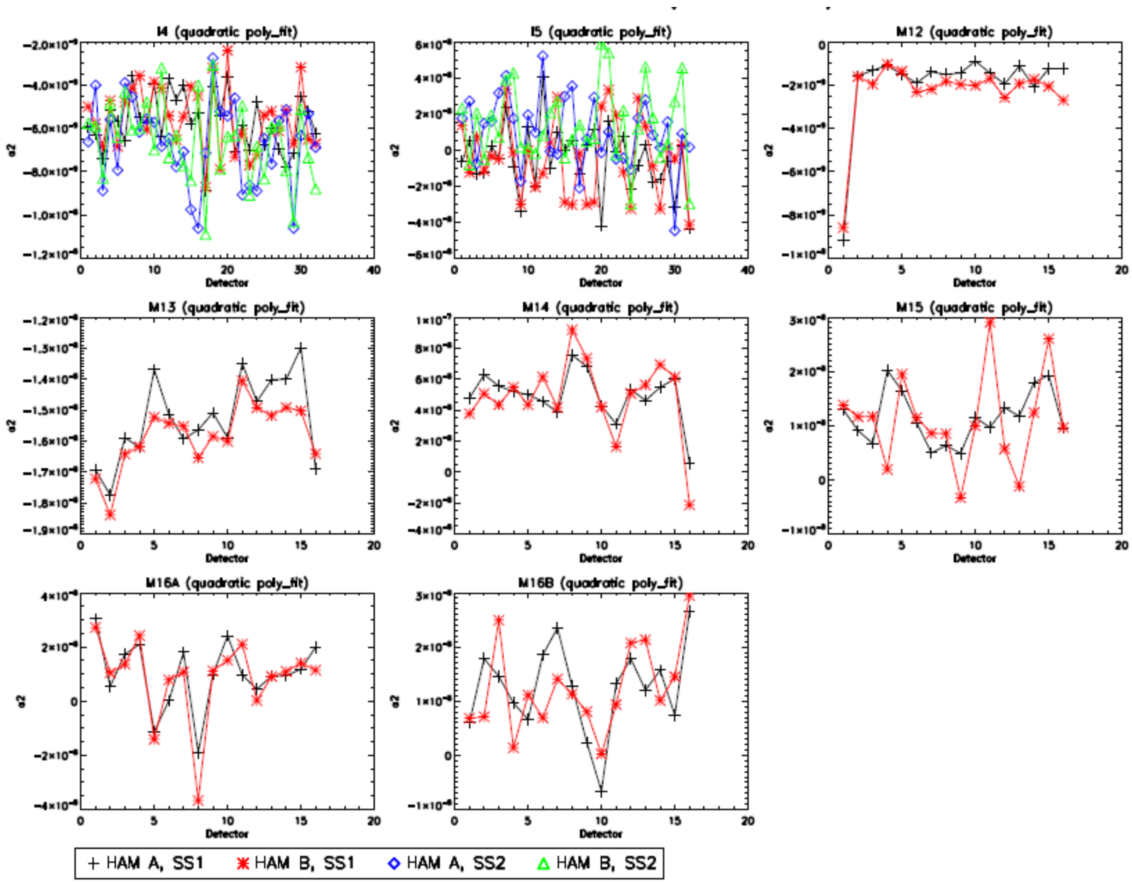

Figure 13: NEdT at T_{TYP} for high gain bands (warm up)

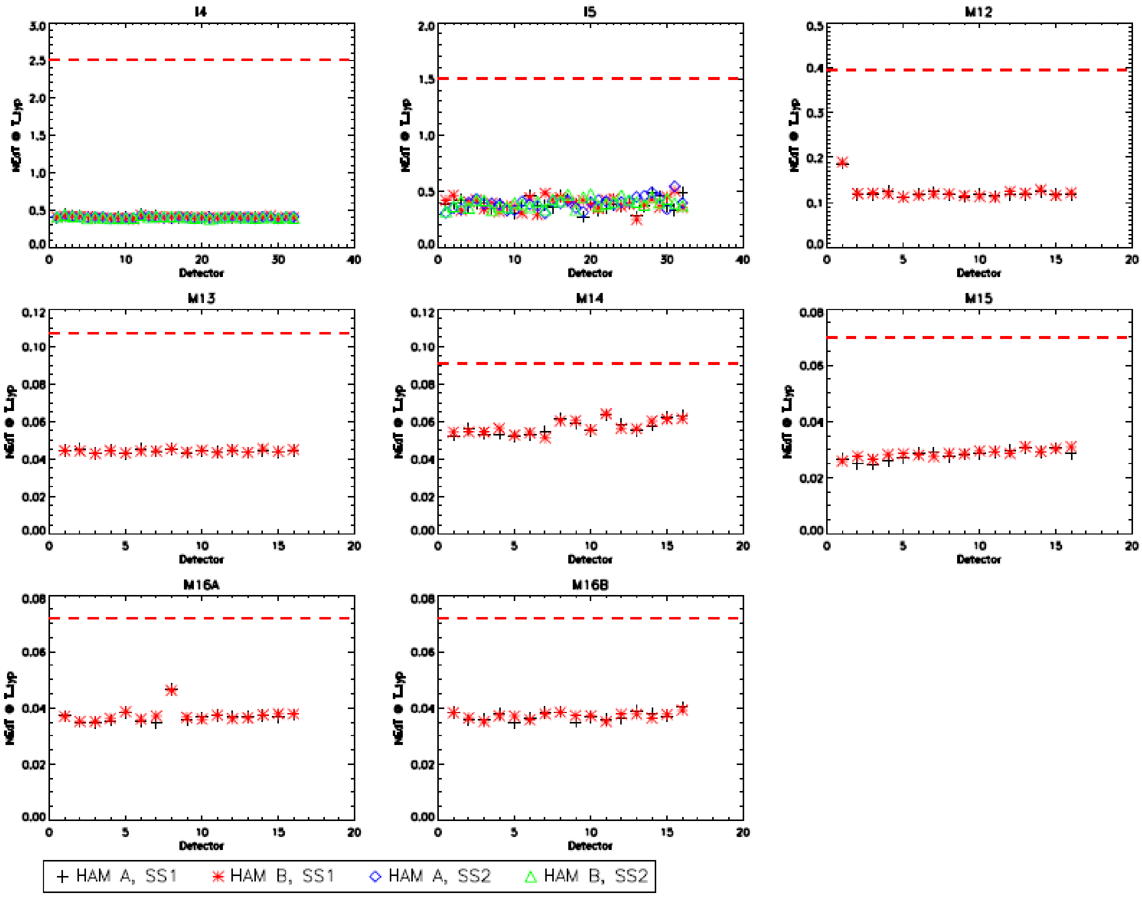

Figure 14: NEdT at T_{TYP} for high gain bands (cool down)

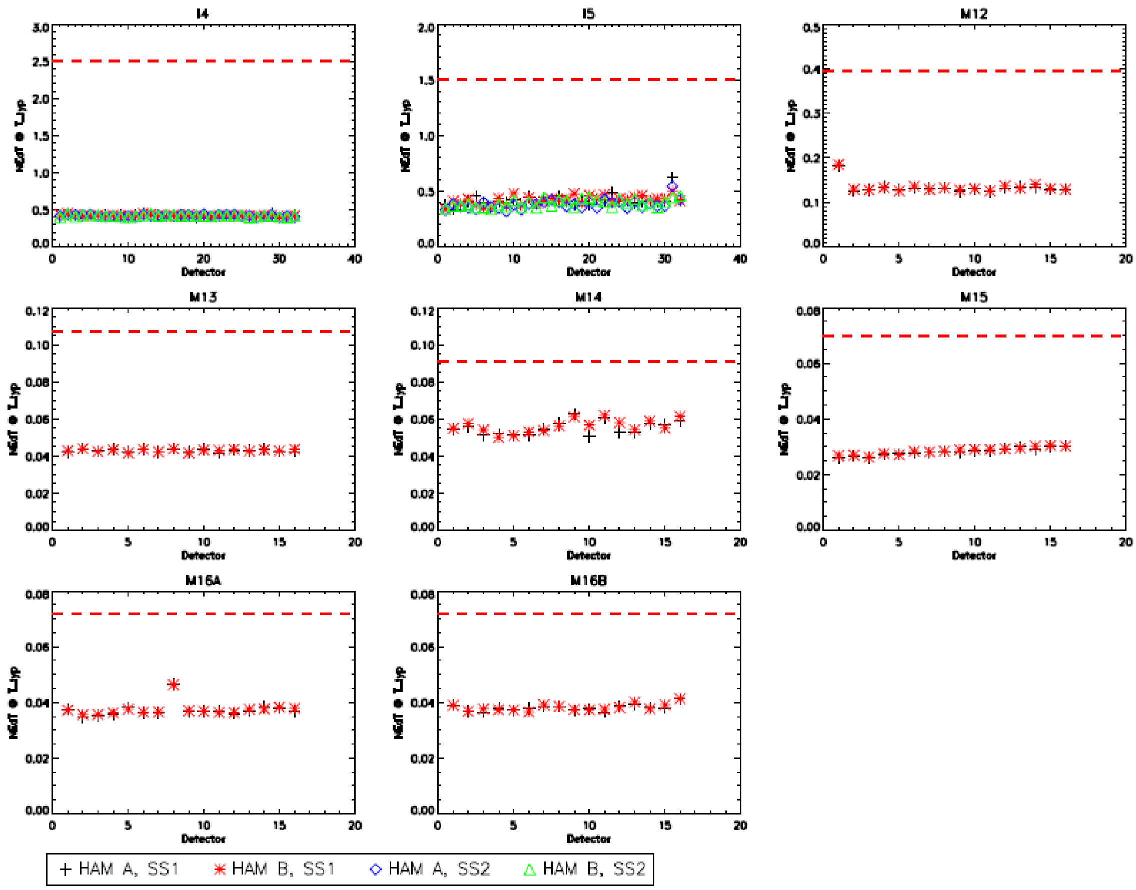

Figure 15: BCS ARD for high gain bands (warm up and cool down)

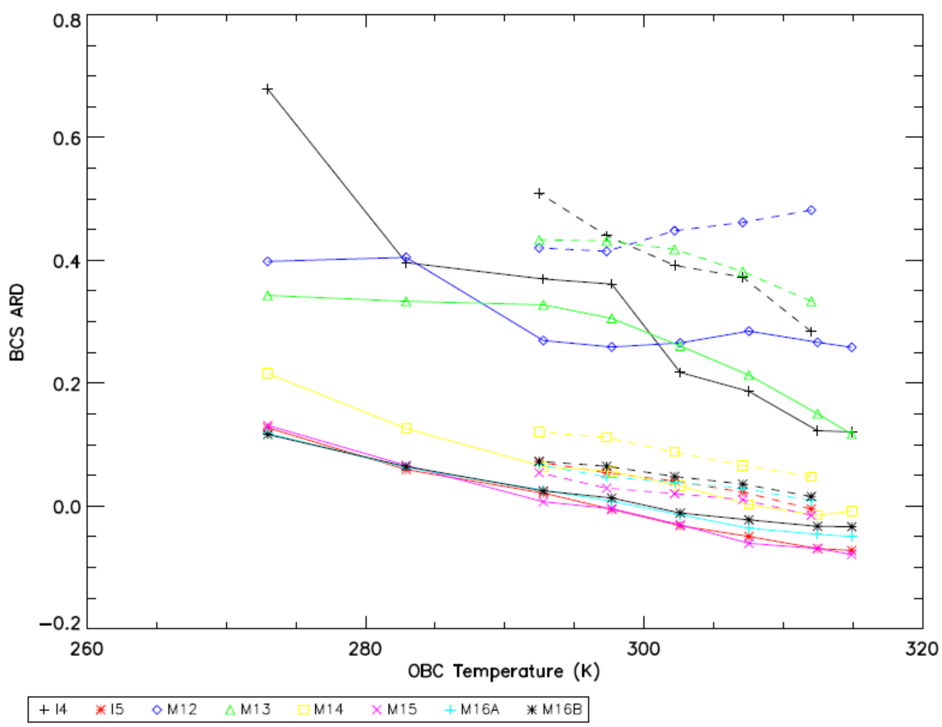

Figure 16: BCS RRU for high gain bands (warm up and cool down)